Published in final edited form as:
Spine J. 2013 November ; 13(11): . doi:10.1016/j.spinee.2013.04.004.

Fullerol nanoparticles suppress inflammatory response and adipogenesis of vertebral bone marrow stromal cells–A potential novel treatment for intervertebral disc degeneration

Qihai Liu, PhD, **Li Jin, MD, PhD**, **Francis H. Shen, MD**, **Gary Balian, PhD**, and **Xudong Joshua Li, MD, PhD***
Department of Orthopedic Surgery, University of Virginia Health System, Charlottesville, Virginia, United States of America

Introduction

Low back pain is a common problem that affects a large proportion of the population at some point, thus carrying an enormous socio-economic burden. Although there are many causes of back pain, symptomatic intervertebral disc (IVD) degeneration also contributes to spinal arthritis, myelopathy, and radioculopathy, and, is strongly implicated as a cause of low back pain [1, 2]. Chronic disc degeneration often requires surgery that alleviates the symptoms without treating the underlying problem, and may lead to biomechanical harm and accelerated degeneration of the adjacent segments [3]. Biological treatment strategies may circumvent these problems. Supplementation with therapeutic proteins, such as growth factors, has been extensively investigated as a stimulus for cell proliferation and extracellular matrix production in the IVD [4–6]. Most therapeutic agents either in clinical trials or laboratory researches have targeted the IVD for treatment, however, few scientists have directed their attention towards the adjacent vertebral body.

Due to their proximity to one another, the IVD has a very close relationship with vertebral bone marrow and they are separated by an endplate, a thin layer which has an osseous as well as a cartilage component [7]. The inflammatory alteration of bone marrow in the vertebral body is associated with disc degeneration. Three types of vertebral bone marrow lesions noted on MRI were first described by Modic et al. in 1988 [8]. Type II changes showed increased signal intensity on T1-weighted images and an iso- or slightly hyperintense signal on T2, which correlated with fatty marrow replacement and inflammatory edema. On the other hand, mature discs almost totally rely on diffusion of essential solutes through the marrow contact channels in the vertebral endplate for nutrition and metabolic exchange [7, 9]. Thus, reduced nutrient is another factor that is implicated in the initiation and progression of the degenerative cascade in the disc [10]. The focal fatty marrow conversion from normal red hemopoietic bone marrow [11] might obstruct the nutrient transport from bone marrow to endplate. Moreover, the growth of fat cells and inflammatory edema in the rigid intraosseous compartment can increase pressure and compress vessels, further decreasing blood flow [12, 13]. Therefore, we hypothesize that

*Corresponding Author: Xudong Joshua Li, Mailing address: Orthopedic Research Laboratories, Box 800374, University of Virginia School of Medicine, Charlottesville, VA 22908, lixudong@virginia.edu, Phone: 434-982-4135, Fax: 434-982-1691.

inhibition of inflammatory mediators and adipogenesis of vertebral bone marrow stromal cells (vBMSCs) may retard the progression of disc degeneration.

While production of reactive oxygen species (ROS) is a consequence of basal cellular respiration, increased ROS production is associated with several pathological conditions including cellular inflammatory responses [14, 15]. Moreover, the regulation of ROS may also contribute to the ultimate fate of cells. It has been reported that increased ROS production is associated with the differentiation of pre-adipocytes to adipocytes, as well as fat tissue accumulation [16]. Thus, effective relief of cellular oxidative stress under inflammatory environment would block ROS-induced adipogenesis [17].

Recently, the anti-oxidative features of fullerene (C60), and its derivatives, have drawn a great deal of attention. Fullerene is composed of 60 carbon atoms with a unique case structure. It has unusual redox chemistry and may be reversibly reduced by up to six electrons, while up to 34 methyl radicals could be added onto a single C60 molecule [18]. Thus, fullerene has been characterized as a “free radical sponge”, with an anti-oxidative efficacy of several hundred-fold higher than conventional antioxidants [19]. Fullerene and its derivatives were found to be in many biological applications: inhibition of nitric oxide formation by suppressing nitric oxide synthase [20], prevention of ischemia-induced injuries in brain [21], inactivation of viruses [22] and prevention of quartz-induced neutrophilic inflammation in the lungs [23]. Furthermore, a Japanese group showed that a water-soluble fullerene prevented the development of cartilage degeneration and arthritis with no detectable toxicity when intraarticularly injected into rabbits of an osteoarthritis model [24].

In this study, we investigated the anti-inflammatory effects of fullerol, a water-soluble, biocompatible fullerene derivative with excellent efficiency in eliminating free radicals [25] to determine the effects on vBMSCs. This study is designed in an attempt to answer two questions. 1) Does fullerol protect vBMSCs from interleukin-1 β (IL-1 β)-induced inflammatory responses by inhibiting matrix metalloproteinases (MMPs) and TNF-α production? 2) Will fullerol inhibit the adipogenic differentiation of vBMSCs? We hypothesize that fullerol has beneficial effects on the two major lesions in vertebral bone marrow: inflammatory alteration and fatty replacement.

Materials and Methods

Isolation of vBMSCs from vertebral bodies of Swiss Webster mice

Animal protocols were approved by the Institutional Animal Care & Use Committee at University of Virginia. The vBMSCs were isolated from vertebrae of five male Swiss Webster mice of one month old (Harlan Laboratories, Wilmington, MA). Mice were sacrificed by CO_2 asphyxiation which was followed by cervical dislocation. The entire spine was dissected out free of muscle and connective tissue. Bone marrow was scooped out with a 18G needle and extruded from vertebrae with low glucose Dulbecco’s modified Eagle’s medium (LG-DMEM, Invitrogen, USA) supplemented with 100 μg/mL streptomycin and 100 U/mL penicillin. After centrifugation at 600 g for 10 min, the pellet was resuspended in growth medium (GM, LG-DMEM supplemented with 10% fetal bovine serum, (FBS, Invitrogen, USA), 100 μg/mL streptomycin, 100 U/mL penicillin) and plated at 1×10^4 cells/cm^2 in 25-cm^2 culture flasks (Falcon, USA). Cells at passage 1 were used in the following studies.

Cytotoxicity of fullerol on vBMSCs

Classically, cytotoxicity is determined by assessment of plasma membrane damage. As lactate dehydrogenase (LDH) is a stable cytoplasmic enzyme present in all cells and rapidly released into culture medium upon damage of the plasma membrane, we quantified the

potential short-term (within 24h) cytotoxicity of fullerol at different concentrations using an LDH-Cytotoxicity Assay Kit (Biovision, USA). To reduce background absorbance generated by phenol red in medium and to minimize possible LDH in FBS, phenol red free DMEM (Invitrogen, USA) supplemented with 1% FBS was used as the assay medium. The salt form of fullerol was purchased from Materials and Electrochemical Research Corporation (Tucson, AZ, USA). The vBMSCs were seeded at a density of 2×10^4 cells/cm^2 in 24-well culture plates and supplemented with 0 (low control), 0.1, 1, and 10 μM fullerol, or 0.5% Triton X-100 (high control). After 6, 12, 18 and 24h of culture, media were harvested for LDH measurement. Absorbance was measured spectrophotometrically at 495 nm and reference wavelength was set at 650 nm. Wells without cells were assayed as the blank controls that were then subtracted from the corresponding samples.

WST-1 assay was performed to evaluate the cytotoxicity of fullerol at longer time (within 7d) by measuring the overall activity of mitochondrial dehydrogenases in viable vBMSCs using Roche WST-1 Kit (Roche Applied Science, Germany). WST-1 assay has been proved to be more sensitive and stable than the traditional MTT, XTT, or MTS assay to detect cellular proliferation or cytotoxicity. The vBMSCs were seeded at a density of 2×10^4 cells/cm^2 in 96-well culture plates and cultured with GM supplemented with 0, 0.1, 1, and 10 μM fullerol. After 0, 1, 3, 5 and 7d of culture, the WST-1 reagent was added to the culture media and incubated for another 3h at 37°C and 5% CO_2. Absorbance of the supernatant was measured spectrophotometrically at 440 nm and reference wavelength was set at 650 nm. Wells without cells were assayed as the blank controls that were then subtracted from the corresponding samples.

Intracellular reactive oxygen species (ROS) detection by fluorescence and flow cytometry analysis

The vBMSCs were cultured in 6-well plates with growth medium (GM), GM+1 μM fullerol, GM+10 ng/mL IL-1 β (Abcam, USA), or GM+1 μM fullerol+10 ng/mL IL-1 β. At day 3, the cells were cultured with LG-DMEM containing 10 μM H_2DCFDA (Invitrogen, USA) in the dark for 30 minutes. Cells were then washed twice with PBS and the green fluorescence was observed under an Olympus fluorescence microscope.

As for flow cytometry analysis, cells were trypsinized and collected by centrifugation. Cells were then incubated with LG-DMEM containing 10 μM H_2DCFDA at 37°C in the dark for 30 min, washed twice with PBS and mean fluorescence intensity (MFI) was measured by flow cytometry. Cells without H_2DCFDA incubation were used as blank control.

MMP-3 and MMP-13 immunofluorescence staining

The vBMSCs were cultured on coverslips in 6-well plates with GM, GM+1μM fullerol, GM +10 ng/mL IL-1 β, or GM+1 μM fullerol+10 ng/mL IL-1 β. At day 3, cells were fixed with ice-cold 4% paraformaldehyde for 15 min followed by incubation with PBS containing 0.25% Triton X-100 for 10 min. After blocking with 1% BSA in PBST for 30 min, goat anti-mouse MMP-3 (Abcam, USA) or MMP-13 (Santa Cruz Biotechnology, USA) primary antibodies were applied (1:1000 dilution) at 4°C overnight followed by incubation with fluoresce in isothiocyanate (FITC)-conjugated donkey anti-goat IgG (Santa Cruz Biotechnology, USA). Nuclei were counter-stained with 50 μg/ml propidium iodide. Immunofluorescence images were taken under an Olympus fluorescence microscope.

Adipogenic differentiation of vBMSCs and fullerol treatment

The vBMSCs were cultured with adipogenic medium (AM) containing GM supplemented with 0.5 mM isobutyl-methylxanthine (IBMX, Sigma, USA), 1 μM dexamethasone (Sigma,

USA), 10 μg/mL insulin (Sigma, USA), and 100 μM indomethacin (Sigma, USA). Under GM or AM culture, vBMSCs were treated with or without 1 μM fullerol.

Oil Red O staining and quantification

After 2 weeks of culture, cellular adipogenic differentiation was assessed by Oil Red O staining to detect the presence of intracellular lipid-filled droplets. Briefly, monolayer cells were fixed in 4% formaldehyde, washed in water and stained with a 0.5% (w/v) Oil Red O (Sigma, USA) solution (60% isopropanol, 40% water) for 15 min at room temperature, rinsed twice with deionized water and adipogenic differentiation was evaluated microscopically.

For quantification of intracellular lipid droplet-stained Oil Red O, cells were washed intensively with deionized water to remove unbound dye, and then isopropanol was added to the stained culture dish. After 10 min of incubation with agitation on an orbital shaker (60 rpm), absorbance of the extract was assayed by a spectrophotometer at 510 nm.

ROS detection by NBT assay during adipogenic differentiation

The vBMSCs were cultured with GM, GM+1 μM fullerol, AM, or AM+1 μM fullerol for 2 weeks. In each group, ROS production was evaluated by nitroblue tetrazolium (NBT, Sigma, USA) assay [16]. Culture media were aspirated and cells were incubated in PBS containing 0.2% NBT at 37°C in the dark for 60 min. NBT was reduced by ROS to a dark-blue, insoluble form of NBT called formazan which could be visualized. For quantification, formazan was dissolved in 50% acetic acid solution by sonication, and absorbance was determined at 560 nm.

RNA extraction and reverse transcription (RT)

Total RNA was extracted using the RNeasy Mini Kit (QIAGEN, Valencia, CA) according to the specification. The concentration of RNA was determined from the optical absorbance at 260 nm of the extract. Complementary DNA (cDNA) was synthesized using the iScript cDNA Synthesis Kit (Bio-Rad, Hercules, CA) according to the manufacturer's instructions.

Quantitative real-time PCR

Real-time PCR was performed with iQ™ 5 multicolor real-time PCR Detection System (Bio-Rad, USA) as previously described [26]. The following genes were evaluated: MMP-1, 3, 13, TNF-α, peroxisome proliferators-activated receptor gamma (PPARγ), and fatty acid-binding protein (aP2). 18S rRNA was used as an internal control to normalize the signal from genes of interest. Sequences of primers, individual annealing temperature and amplicon lengths are shown in Table 1.

Statistical analysis

All experiments were performed in triplicate and data were presented as mean ± standard deviation (SD). Statistical analyses for quantitative assays were performed by One-Way ANOVA assuming equal variance (Student-Newman-Keul (S-N-K) test) using SPSS 11.0 software. A *p*-value of less than 0.05 was considered statistically significant.

Results

Cytotoxicity of fullerol on vBMSCs

To detect the acute cytotoxicity of fullerol, we measured the LDH leakage into culture media. As shown in Fig. 1A, at 18h, the 10 μM fullerol group showed significant cytotoxicity compared with culture medium only (0 μM fullerol), and by 24h, cytotoxicity in

this group was significantly higher than that in the 1 μM fullerol group. However, fullerol at dose of 0.1 or 1 μM exhibited no statistical difference compared with culture medium only during the observed time period. For the long-time cytotoxicity detection, we performed WST-1 assay. As shown in Fig. 1B, during the 7d-culture period, only 10 μM fullerol group showed significant cytotoxicity compared with GM only (0 μM fullerol) beginning after 1d. There was no statistical difference among the other groups at each time point. Thus, fullerol at a concentration of 1 μM was used in the following studies.

Fullerol suppressed intracellular ROS

To evaluate the anti-oxidative effects of fullerol, we performed both fluorescence staining and flow cytometry analysis to measure intracellular ROS. As shown in Fig. 2, the positively stained cells (colored green) increased in the IL-1 β-treated group compared with the non-treated group, but decreased in the corresponding fullerol group. Quantification with flow cytometry confirmed this observation. Fullerol significantly suppressed both basal and IL-1 β-induced intracellular ROS, with 23% and 18% reduction, respectively.

Anti-inflammatory effects of fullerol on vBMSCs

First, we performed immunofluorescence staining to measure cellular expression of two typical members of the MMP family, MMP-3 (stromelysin 1) and MMP-13 (collagenase 3). As shown in Fig. 3A, after 3 days of culture, basal expression of MMP-3 and MMP-13 were low in cells with or without fullerol treatment, while fullerol significantly inhibited the expression of MMP-3 and MMP-13 induced by pro-inflammatory cytokine IL-1 β. We further confirmed this observation at the molecular level. As shown in Fig. 3B, the mRNA levels of MMP-1, 3, 13 were markedly increased by IL-1 β stimulation, while fullerol suppressed this elevation by 26–36% ($p<0.05$). Additionally, fullerol also inhibited the expression of pro-inflammatory cytokine TNF-α by 33% ($p<0.05$) in IL-1 β-treated groups.

Fullerol inhibited vBMSC adipogenesis through elimination of ROS

To investigate whether fullerol could retard adipogenic differentiation of vBMSCs, we evaluated both intracellular lipid-filled droplet formation and adipogenic gene expression. As demonstrated in Fig. 4A, after 2 weeks of culture, there was little lipid droplet formation in both GM and GM+fullerol groups as detected by Oil Red O staining. Under adipogenic induction, intensive lipid droplets were formed in cells, and fullerol attenuated cellular adipogenesis dramatically by 28% as shown by the relative quantification data for Oil Red O content. Real-time PCR results (Fig. 4B) showed that fullerol significantly decreased the expression of adipogenic genes PPARγ (early-mid marker) and aP2 (mid-late marker), by 19% and 69%, respectively, in the AM-treated groups.

Moreover, to further elucidate whether fullerol suppressed vBMSC adipogenesis through ROS scavenging, we measured ROS content in parallel with the NBT assay (Fig. 5). The most intensive signal was detected in the adipogenic induction group, and was weakened dramatically by fullerol. In control groups with or without fullerol treatment, the cells showed little ROS expression. The relative quantification result was consistent with the observations with staining.

Discussion

IVD degeneration is one of the risk factors for chronic low back pain. As the vertebra is a nutrient resource, vertebral bone marrow abnormalities were observed in IVD degeneration disease. The cause and effect relationship between vertebral damage and disc degeneration is still a mystery.

Magnetic resonance signal intensity changes were observed in vertebral bone marrow adjacent to the endplates in 50% of IVD degeneration cases [11]. Data from multiple independent studies [27–29] suggested that Modic Type I and II adjacent to the endplate are among the most specific of all MRI observations for predicting concordant pain with discography. All these studies suggested that adjacent bone marrow abnormalities may cause discogenic back pain. One important question is whether the discogenic back pain could be attenuated by treating the adjacent bone marrow lesion. In this study, we demonstrated that fullerol, a potent antioxidant agent, suppressed IL-1 β-induced inflammatory changes of vBMSCs and inhibited the adipogenic differentiation of vBMSCs. Thus, fullerol may be considered for further investigation as a therapeutic agent to reverse inflammatory and fatty degenerative lesions in vertebral bone marrow and possibly to further retard IVD degenerative changes.

Since its first detection and bulk production, fullerene and its derivatives have gained a prime role on the scientific scene [20–24, 30]. Herein, we demonstrated that fullerol, a polyhydroxylated fullerene derivative, inhibited IL-1 β-induced production of inflammatory mediators such as MMPs and TNF-α (Fig. 3). In vBMSCs, the elevation of MMP-1, 3, 13 and TNF-α mRNA levels initiated by pro-inflammatory cytokine IL-1 β was significantly suppressed by administration of 1 μM fullerol. Immunofluorescence staining also confirmed the expression change of MMP-3 and 13. As IL-1 β plays a crucial role in the induction of degradative metabolic events, IL-1 β stimulation is commonly used as a tool to mimic inflammation [31]. MMPs are a family of zinc-dependent endopeptidases degrading all the main protein components of the extracellular matrix and thus play an essential role in tissue remodeling and repair associated with development and inflammation [32, 33]. The activity of MMPs is regulated by pro-inflammatory cytokines such as interleukins and TNF-α, and MMP inhibitors TIMPs [34], and this control is fundamental in controlling the inflammatory state. Park et al. [35] suggested that oxidative stress may trigger cellular inflammation signals, such as TNF-α pathway. TNF-α is one of the major mediators of inflammation; through a wide range of pathogenic stimuli, TNF-α induces other inflammatory mediators and proteases that orchestrate inflammatory responses [36]. We demonstrated that fullerol significantly decreased IL-1 β-induced ROS level in vBMSCs as measured by ROS staining and flow cytometry assays (Fig. 2), which may account for the decreased expression of MMPs and TNF-α. This is consistent with a previous study which showed that oxidative stress activated several pro-inflammatory and pro-apoptotic pathways [37].

The BMSCs have both osteogenic and adipogenic differentiation potentials in vitro [38, 39] and in vivo [40, 41]. It is well accepted that there exists a reciprocal balance between osteogenesis and adipogenesis of BMSCs [42], and disturbance of such balance would be associated with physiologic disorders, characterized by an increase of adipocytes in bone marrow. The focal fatty degeneration in bone marrow adjacent to the endplate of discs would block the transport of nutrients and metabolic exchange, essential for discs, and thus contribute to disc degeneration. Therefore, we hypothesized that fullerol could inhibit adipogenesis of vBMSCs and thereby prevent fatty deposition in vertebral bone marrow. Indeed, we found that fullerol dramatically retarded the adipogenic differentiation of vBMSCs. With 1 μM fullerol treatment, the lipid droplets decreased by 28% in vBMSCs fed with adipogenic medium as revealed by Oil Red O staining assay (Fig. 4A). In addition, the expression of adipogenic specific genes PPARγ and aP2 were both downregulated. PPARγ is regarded as a master regulator of adipogenic differentiation and is involved in the transcriptional control of many different genes involved in adipogenesis [43], the transcriptional cascades of which lead to the expression of the proteins and enzymes that are essential for lipogenesis. Fatty acid–binding protein aP2 regulates systemic glucose and lipid metabolism [44], and is associated with lipid accumulation within mature adipocytes [45]. Interestingly, we found that fullerol suppressed aP2 expression (by 69%) much more than it

did on PPARγ expression (by 19%) at 2 weeks. One explanation is that PPARγ is an early-to-mid marker for adipogenic differentiation, and aP2 is a mid-to-late marker for adipogenic differentiation. After 2 weeks of adipogenic induction, the expression of PPARγ may have already dropped down from its peak level. Nevertheless, fullerol prohibited cellular adipogenic differentiation by inhibiting both early-to-mid and mid-to-late adipogenic marker gene expression. What is the reason for the effect of fullerol in suppressing cellular adipogenesis? It was revealed that elevation of ROS production is associated with the differentiation of pre-adipocytes to adipocytes [16]. Using the NBT assay to evaluate the level of ROS, we found that the adipogenic induction group had the highest signal, while it was dramatically weakened with the administration of fullerol. Therefore, we considered that the suppression of adipogenesis by fullerol may be attributed to the reduction of ROS.

Although fullerol is not genotoxic [46], it was reported that a maximal dose (100 μg/ml, approximate 88.7 μM) of fullerol induced cytotoxic injury on human endothelial cells [47] and was cytotoxic to human lens epithelial cells at concentrations higher than 20 μM [48]. These suggest that the cytotoxicity of fullerol is cell type dependant. Two processes may account for the observed phenomena. First, during the process of cellular uptake, fullerol may cause damage to the cell membrane and organelles. Second, although fullerol is a “free radical sponge”, the photoexcitation of fullerene derivatives efficiently produces an excited triplet state and, through energy and electron transfer to molecular oxygen, produce both singlet molecular oxygen and superoxide which may injure cells [48]. The balance between ROS scavenging and production mediates its cytoprotection or photo-cytotoxicity on cells. We performed both LDH leakage assay and WST-1 assay to investigate short-term and relatively long-term cytotoxicity of fullerol. We found significantly higher cytotoxicity of 10 μM fullerol after 24h of culture, and there was no significant difference among the ≤1 μM (0.1 and 1 μM) and low control (0 fullerol) groups (Fig. 1) during the 7d-culture period. Therefore, we used 1 μM fullerol in our study. However, in the following in vivo study, local injection of fullerol into vertebral body in a mouse disc degeneration model, we will rigorously test the dose window of fullerol to maximize its anti-oxidative and anti-inflammatory effects, as well as minimize the side effects.

In conclusion, we believe that this is the first observation that fullerol, a potent antioxidant agent, suppresses IL-1 β-induced ROS and inflammatory cytokine production, inhibits the adipogenic differentiation of vBMSCs in vitro and, therefore, may prevent vertebral fatty marrow deposition and inflammatory responses during disc degeneration. One important concept raised in this study is that in addition to direct treatment of IVD for disc degeneration, we could rectify the lesions in vertebral bone marrow, which eventually would facilitate IVD treatment. However, this treatment strategy requires further investigation both in vitro and in vivo. We propose that further studies with fullerol may be lead to the development of an effective agent for the treatment of symptomatic IVD degeneration.

References

1. Freemont AJ. The cellular pathobiology of the degenerate intervertebral disc and discogenic back pain. Rheumatology (Oxford). 2009; 48:5–10. [PubMed: 18854342]
2. Risbud MV, Albert TJ, Guttapalli A, Vresilovic EJ, Hillibrand AS, Vaccaro AR, et al. Differentiation of mesenchymal stem cells towards a nucleus pulposus-like phenotype in vitro: implications for cell-based transplantation therapy. Spine (Phila Pa 1976). 2004; 29:2627–32. [PubMed: 15564911]
3. Orozco L, Soler R, Morera C, Alberca M, Sanchez A, Garcia-Sancho J. Intervertebral disc repair by autologous mesenchymal bone marrow cells: a pilot study. Transplantation. 2011; 92:822–8. [PubMed: 21792091]

4. Masuda K. Biological repair of the degenerated intervertebral disc by the injection of growth factors. European spine journal : official publication of the European Spine Society, the European Spinal Deformity Society, and the European Section of the Cervical Spine Research Society. 2008; 17 (Suppl 4):441–51.
5. Li X, Leo BM, Beck G, Balian G, Anderson GD. Collagen and proteoglycan abnormalities in the GDF-5-deficient mice and molecular changes when treating disk cells with recombinant growth factor. Spine (Phila Pa 1976). 2004; 29:2229–34. [PubMed: 15480133]
6. Cui M, Wan Y, Anderson DG, Shen FH, Leo BM, Laurencin CT, et al. Mouse growth and differentiation factor-5 protein and DNA therapy potentiates intervertebral disc cell aggregation and chondrogenic gene expression. The spine journal : official journal of the North American Spine Society. 2008; 8:287–95. [PubMed: 17974491]
7. Moore RJ. The vertebral endplate: disc degeneration, disc regeneration. European spine journal : official publication of the European Spine Society, the European Spinal Deformity Society, and the European Section of the Cervical Spine Research Society. 2006; 15 (Suppl 3):S333–7.
8. Modic MT, Masaryk TJ, Ross JS, Carter JR. Imaging of degenerative disk disease. Radiology. 1988; 168:177–86. [PubMed: 3289089]
9. Wang Y, Battie MC, Boyd SK, Videman T. The osseous endplates in lumbar vertebrae: thickness, bone mineral density and their associations with age and disk degeneration. Bone. 2011; 48:804–9. [PubMed: 21168539]
10. Urban JP, Smith S, Fairbank JC. Nutrition of the intervertebral disc. Spine (Phila Pa 1976). 2004; 29:2700–9. [PubMed: 15564919]
11. de Roos A, Kressel H, Spritzer C, Dalinka M. MR imaging of marrow changes adjacent to end plates in degenerative lumbar disk disease. AJR American journal of roentgenology. 1987; 149:531–4. [PubMed: 3497539]
12. Wang GJ, Sweet DE, Reger SI, Thompson RC. Fat-cell changes as a mechanism of avascular necrosis of the femoral head in cortisone-treated rabbits. J Bone Joint Surg Am. 1977; 59:729–35. [PubMed: 908695]
13. Drescher W, Li H, Qvesel D, Jensen SD, Flo C, Hansen ES, et al. Vertebral blood flow and bone mineral density during long-term corticosteroid treatment: An experimental study in immature pigs. Spine (Phila Pa 1976). 2000; 25:3021–5. [PubMed: 11145813]
14. Hatanaka E, Dermargos A, Armelin HA, Curi R, Campa A. Serum amyloid A induces reactive oxygen species (ROS) production and proliferation of fibroblast. Clin Exp Immunol. 2011; 163:362–7. [PubMed: 21175596]
15. Naha PC, Davoren M, Lyng FM, Byrne HJ. Reactive oxygen species (ROS) induced cytokine production and cytotoxicity of PAMAM dendrimers in J774A.1 cells. Toxicol Appl Pharmacol. 2010; 246:91–9. [PubMed: 20420846]
16. Furukawa S, Fujita T, Shimabukuro M, Iwaki M, Yamada Y, Nakajima Y, et al. Increased oxidative stress in obesity and its impact on metabolic syndrome. The Journal of clinical investigation. 2004; 114:1752–61. [PubMed: 15599400]
17. Xiao L, Aoshima H, Saitoh Y, Miwa N. The effect of squalane-dissolved fullerene-C60 on adipogenesis-accompanied oxidative stress and macrophage activation in a preadipocyte-monocyte co-culture system. Biomaterials. 2010; 31:5976–85. [PubMed: 20488530]
18. Bakry R, Vallant RM, Najam-ul-Haq M, Rainer M, Szabo Z, Huck CW, et al. Medicinal applications of fullerenes. International journal of nanomedicine. 2007; 2:639–49. [PubMed: 18203430]
19. Krusic PJ, Wasserman E, Keizer PN, Morton JR, Preston KF. Radical reactions of c60. Science. 1991; 254:1183–5. [PubMed: 17776407]
20. Wolff DJ, Papoiu AD, Mialkowski K, Richardson CF, Schuster DI, Wilson SR. Inhibition of nitric oxide synthase isoforms by tris-malonyl-C(60)-fullerene adducts. Archives of biochemistry and biophysics. 2000; 378:216–23. [PubMed: 10860539]
21. Lin AM, Fang SF, Lin SZ, Chou CK, Luh TY, Ho LT. Local carboxyfullerene protects cortical infarction in rat brain. Neuroscience research. 2002; 43:317–21. [PubMed: 12135775]

22. Rud Y, Buchatskyy L, Prylutskyy Y, Marchenko O, Senenko A, Schutze C, et al. Using C60 fullerenes for photodynamic inactivation of mosquito iridescent viruses. Journal of enzyme inhibition and medicinal chemistry. 2012; 27:614–7. [PubMed: 21883040]
23. Roursgaard M, Poulsen SS, Kepley CL, Hammer M, Nielsen GD, Larsen ST. Polyhydroxylated C60 fullerene (fullerenol) attenuates neutrophilic lung inflammation in mice. Basic & clinical pharmacology & toxicology. 2008; 103:386–8. [PubMed: 18793270]
24. Yudoh K, Shishido K, Murayama H, Yano M, Matsubayashi K, Takada H, et al. Water-soluble C60 fullerene prevents degeneration of articular cartilage in osteoarthritis via down-regulation of chondrocyte catabolic activity and inhibition of cartilage degeneration during disease development. Arthritis and rheumatism. 2007; 56:3307–18. [PubMed: 17907184]
25. Qingnuan L, yan X, Xiaodong Z, Ruili L, qieqie D, Xiaoguang S, et al. Preparation of (99m)Tc-C(60)(OH)(x) and its biodistribution studies. Nucl Med Biol. 2002; 29:707–10. [PubMed: 12234597]
26. Feng G, Yang X, Shang H, Marks IW, Shen FH, Katz A, et al. Multipotential differentiation of human anulus fibrosus cells: an in vitro study. J Bone Joint Surg Am. 2010; 92:675–85. [PubMed: 20194326]
27. Braithwaite I, White J, Saifuddin A, Renton P, Taylor BA. Vertebral end-plate (Modic) changes on lumbar spine MRI: correlation with pain reproduction at lumbar discography. European spine journal : official publication of the European Spine Society, the European Spinal Deformity Society, and the European Section of the Cervical Spine Research Society. 1998; 7:363–8.
28. Buttermann GR. The effect of spinal steroid injections for degenerative disc disease. The spine journal : official journal of the North American Spine Society. 2004; 4:495–505. [PubMed: 15363419]
29. Sandhu HS, Sanchez-Caso LP, Parvataneni HK, Cammisa FP Jr, Girardi FP, Ghelman B. Association between findings of provocative discography and vertebral endplate signal changes as seen on MRI. Journal of spinal disorders. 2000; 13:438–43. [PubMed: 11052355]
30. Kroto HW, Heath JR, Obrien SC, Curl RF, Smalley RE. C-60 - Buckminsterfullerene. Nature. 1985; 318:162–3.
31. Campo GM, Avenoso A, D'Ascola A, Scuruchi M, Prestipino V, Calatroni A, et al. Hyaluronan in part mediates IL-1beta-induced inflammation in mouse chondrocytes by up-regulating CD44 receptors. Gene. 2012; 494:24–35. [PubMed: 22192912]
32. Sternlicht MD, Werb Z. How matrix metalloproteinases regulate cell behavior. Annual review of cell and developmental biology. 2001; 17:463–516.
33. Egeblad M, Werb Z. New functions for the matrix metalloproteinases in cancer progression. Nature reviews Cancer. 2002; 2:161–74.
34. Mocchegiani E, Giacconi R, Costarelli L. Metalloproteases/anti-metalloproteases imbalance in chronic obstructive pulmonary disease: genetic factors and treatment implications. Current opinion in pulmonary medicine. 2011; 17 (Suppl 1):S11–9. [PubMed: 22209925]
35. Park EJ, Yi J, Chung KH, Ryu DY, Choi J, Park K. Oxidative stress and apoptosis induced by titanium dioxide nanoparticles in cultured BEAS-2B cells. Toxicology letters. 2008; 180:222–9. [PubMed: 18662754]
36. Sethi G, Sung B, Aggarwal BB. TNF: a master switch for inflammation to cancer. Frontiers in bioscience : a journal and virtual library. 2008; 13:5094–107. [PubMed: 18508572]
37. Grimsrud PA, Xie H, Griffin TJ, Bernlohr DA. Oxidative stress and covalent modification of protein with bioactive aldehydes. The Journal of biological chemistry. 2008; 283:21837–41. [PubMed: 18445586]
38. Pittenger MF, Mackay AM, Beck SC, Jaiswal RK, Douglas R, Mosca JD, et al. Multilineage potential of adult human mesenchymal stem cells. Science. 1999; 284:143–7. [PubMed: 10102814]
39. Jones EA, Kinsey SE, English A, Jones RA, Straszynski L, Meredith DM, et al. Isolation and characterization of bone marrow multipotential mesenchymal progenitor cells. Arthritis and rheumatism. 2002; 46:3349–60. [PubMed: 12483742]
40. Dallari D, Fini M, Stagni C, Torricelli P, Nicoli Aldini N, Giavaresi G, et al. In vivo study on the healing of bone defects treated with bone marrow stromal cells, platelet-rich plasma, and freeze-

dried bone allografts, alone and in combination. J Orthop Res. 2006; 24:877–88. [PubMed: 16609976]

41. Crossno JT Jr, Majka SM, Grazia T, Gill RG, Klemm DJ. Rosiglitazone promotes development of a novel adipocyte population from bone marrow-derived circulating progenitor cells. The Journal of clinical investigation. 2006; 116:3220–8. [PubMed: 17143331]
42. Jaiswal RK, Jaiswal N, Bruder SP, Mbalaviele G, Marshak DR, Pittenger MF. Adult human mesenchymal stem cell differentiation to the osteogenic or adipogenic lineage is regulated by mitogen-activated protein kinase. The Journal of biological chemistry. 2000; 275:9645–52. [PubMed: 10734116]
43. Morrison RF, Farmer SR. Hormonal signaling and transcriptional control of adipocyte differentiation. The Journal of nutrition. 2000; 130:3116S–21S. [PubMed: 11110883]
44. Shum BO, Mackay CR, Gorgun CZ, Frost MJ, Kumar RK, Hotamisligil GS, et al. The adipocyte fatty acid-binding protein aP2 is required in allergic airway inflammation. The Journal of clinical investigation. 2006; 116:2183–92. [PubMed: 16841093]
45. Bernlohr DA, Doering TL, Kelly TJ Jr, Lane MD. Tissue specific expression of p422 protein, a putative lipid carrier, in mouse adipocytes. Biochemical and biophysical research communications. 1985; 132:850–5. [PubMed: 2415129]
46. Zakharenko LP, Zakharov IK, Vasiunina EA, Karamysheva TV, Danilenko AM, Nikiforov AA. Determination of the genotoxicity of fullerene C60 and fullerol using the method of somatic mosaics on cells of Drosophila melanogaster wing and SOS-chromotest. Genetika. 1997; 33:405–9. [PubMed: 9244774]
47. Yamawaki H, Iwai N. Cytotoxicity of water-soluble fullerene in vascular endothelial cells. American journal of physiology Cell physiology. 2006; 290:C1495–502. [PubMed: 16407415]
48. Roberts JE, Wielgus AR, Boyes WK, Andley U, Chignell CF. Phototoxicity and cytotoxicity of fullerol in human lens epithelial cells. Toxicol Appl Pharmacol. 2008; 228:49–58. [PubMed: 18234258]

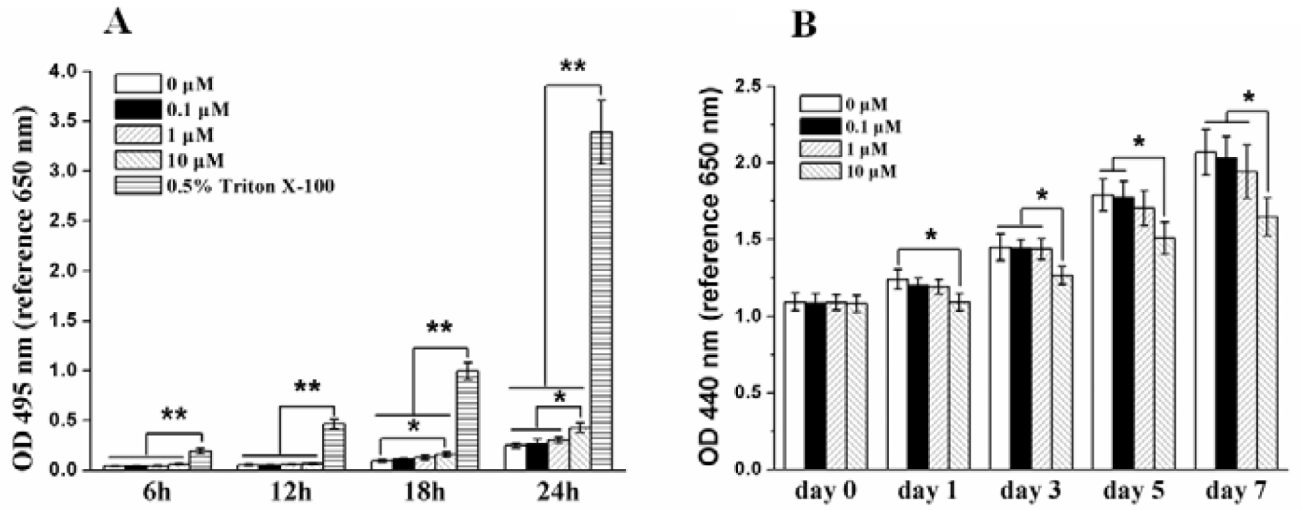

Figure 1.

Cytotoxicity assay of fullerol on mouse vertebral BMSCs (vBMSCs). A: Sub-confluent vBMSCs were cultured in 24-well plates and treated with 0 (low control), 0.1, 1, 10 μM fullerol, or 0.5% Triton X-100 (high control). Media were harvested at 6, 12, 18 and 24h and cellular LDH leakage was measured at OD 495 nm (reference 650 nm). Wells without cells were assayed as blank controls that were then subtracted from the corresponding samples. * $p<0.05$, ** $p<0.01$. B: Sub-confluent vBMSCs were cultured in 96-well plates and treated with 0 (control), 0.1, 1, and 10 μM fullerol up to 7d. WST-1 assay was performed to evaluate the cytotoxicity of fullerol by measuring the overall activity of mitochondrial dehydrogenases in viable vBMSCs. Absorbance of of the supernatant was measured spectrophotometrically at 440 nm (reference 650 nm). Wells without cells were assayed as blank controls that were then subtracted from the corresponding samples. * $p<0.05$.

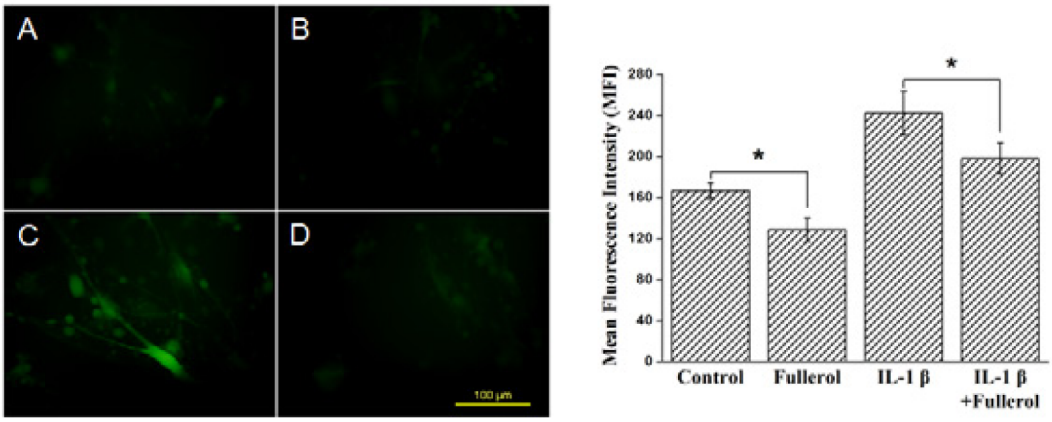

Figure 2.

Fullerol suppressed intracellular ROS. Mouse vertebral BMSCs (vBMSCs) were cultured in 6-well plates with A: growth medium (GM, control), B: GM+1 μM fullerol, C: GM+10 ng/mL interleukin-1 β (IL-1 β), or D: GM+1 μM fullerol+10 ng/mL IL-1 β. At day 3, intracellular ROS intensity was detected by H_2DCFDA fluorescence assay. Bar scale=100 μm. ROS was further quantified with flow cytometry by measuring mean fluorescence intensity (MFI). * $p<0.05$.

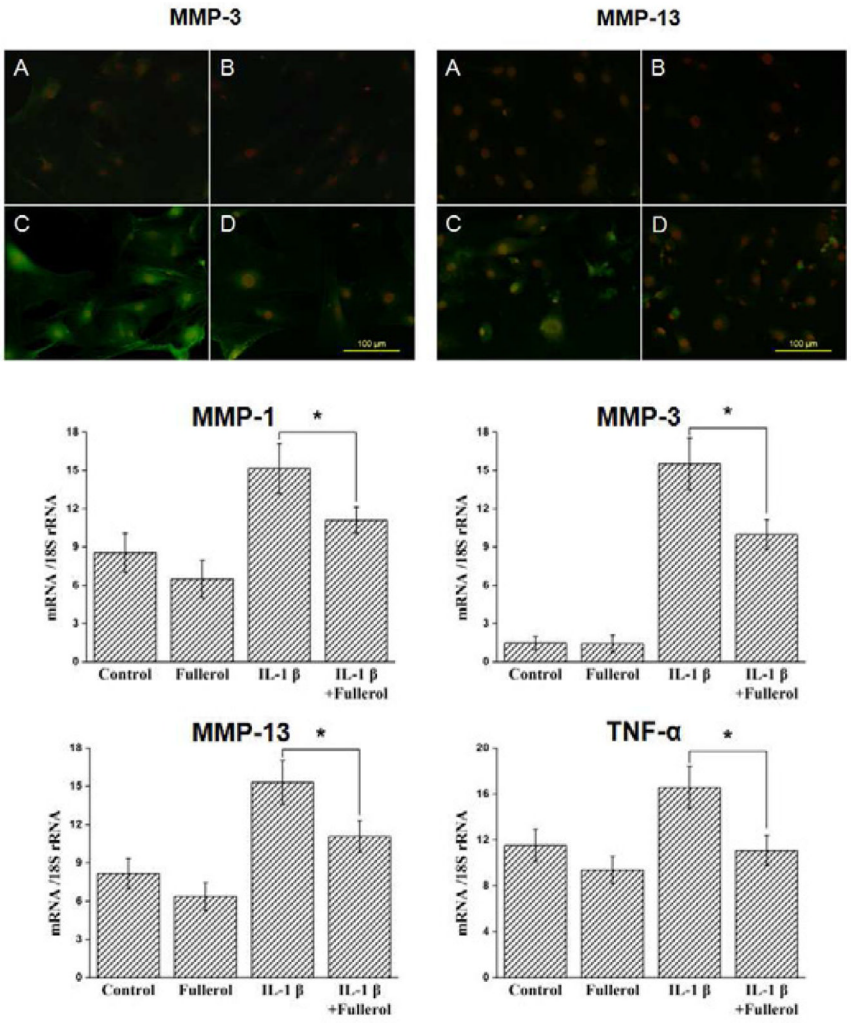

Figure 3.

Fullerol suppressed cellular inflammatory response induced by IL-1 β. Mouse vertebral BMSCs (vBMSCs) were cultured on coverslips in 6-well plates with A: GM (control), B: GM+1 μM fullerol, C: GM+10 ng/mL IL-1 β, or D: GM+1 μM fullerol+10 ng/mL IL-1 β. At day 3, cells were fixed with 4% paraformaldehyde and MMP-3 and 13 antibodies were applied. The proteins were detected with FITC-conjugated IgG (green color). The cells were visualized under a fluorescence microscope. Nuclei were counter-stained with propidium iodide (red color). Bar scale=100 μm. B: At 3 days of culture, total RNA was extracted. Gene expression for MMP-1, 3, 13 and TNF-α was measured by real-time PCR with specific primers. Relative mRNA content was normalized to 18S rRNA. * $p<0.05$.

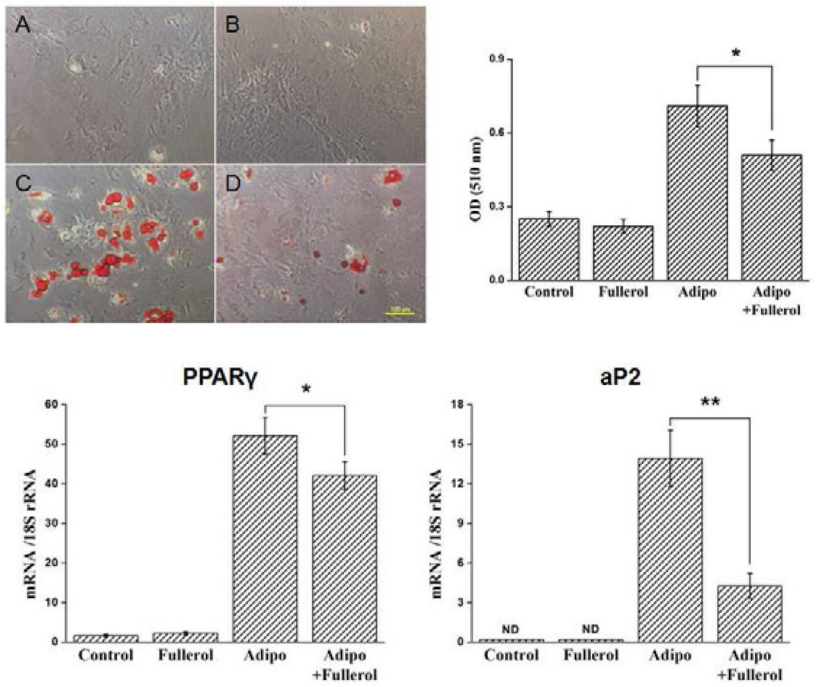

Figure 4.

Fullerol suppressed cellular adipogenic differentiation in vitro. Mouse vertebral BMSCs (vBMSCs) were cultured in 12-well plates with A: GM (control), B: GM+1 μM fullerol, C: adipogenic medium (AM), or D: AM+1 μM fullerol. Two weeks after culture, A: Intracellular lipid-filled droplets were detected by Oil Red O staining. Bar scale=100 μm. Bar graph shows the relative quantification of Oil Red O. B: Total RNA was extracted and gene expressions of PPARγ and aP2 were measured by real-time PCR with specific primers. Relative mRNA content was normalized to 18S rRNA. * $p<0.05$, ** $p<0.01$. "ND" denotes "Non Detectable".

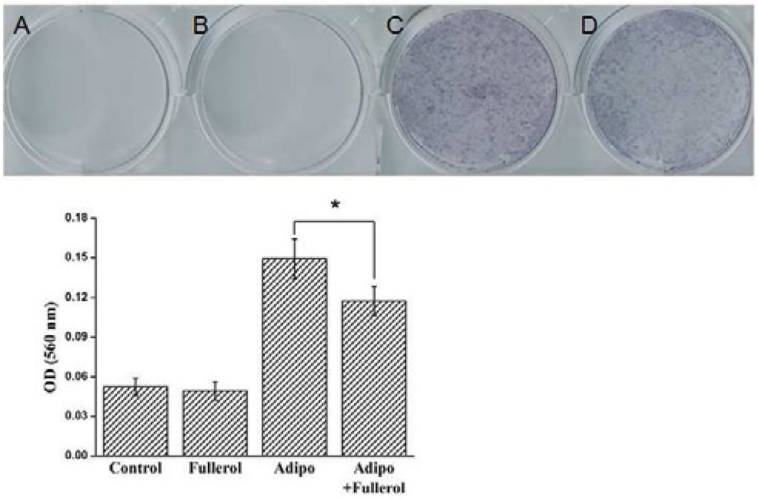

Figure 5.

Fullerol treatment decreased ROS production in parallel with suppression of cellular adipogenic differentiation. Mouse vertebral BMSCs (vBMSCs) were cultured in 12-well plates with A: GM (control), B: GM+1 μM fullerol, C: adipogenic medium (AM), or D: AM +1 μM fullerol. Two weeks after culture, ROS content was evaluated by nitroblue tetrazolium (NBT) assay. NBT was reduced by ROS to a dark-blue, insoluble form of NBT called formazan. For quantification, formazan was dissolved in 50% acetic acid solution by sonication, and absorbance was measured at 560 nm. * $p<0.05$.

Table 1

Sequences of primers and real-time PCR conditions

Gene	Primers (F=forward; R=reverse)	Amplicon size (bp)	Annealing temperature (° C)
MMP-1	F: 5′-ACTCCCTTGGGCTCACTCATT-3′ R: 5′-ATCCTGGTTTAGCACAAAGTCTTCA-3′	92	56
MMP-3	F: 5′-TGATGAACGATGGACAGAGGAT-3′ R: 5′-CTTGAGAGAGATGGAAACGGGA-3′	164	55
MMP-13	F: 5′-TTTCTTTATGGTCCAGGCGAT-3′ R: 5′-TGTTTTGGGATGCTTAGGGTT-3′	51	55
TNF-α	F: 5′-GGCTGCCCCGACTACGT-3′ R: 5′-GACTTTCTCCTGGTATGAGATAGCAA-3′	69	56
PPARγ	F: 5′-GACCACTCGCATTCCTTT-3′ R: 5′-CCACAGACTCGGCACTCA-3′	266	55
aP2	F: 5′-AGTGGGAGTGGGCTTTGC-3′ R: 5′-CCTGTCGTCTGCGGTGAT-3′	169	55
18s	F: 5′-CGGCGACGACCCATTCGAAC-3′ R: 5′-GAATCGAACCCTGATTCCCCGTC-3′	99	58